Conference paper

Robert L. Mnisi, Peter P. Ndibewu* and Ntebogeng S. Mokgalaka

Green Chemistry in action: towards sustainable production of Gold nanoparticles

DOI 10.1515/pac-2015-1001

Abstract: This study reports the synthesis of gold nanoparticles from a gold precursor salt ($HAuCl_4 \cdot 3H_2O$) using *Moringa oleifera* bark broth, a cheap renewable material, without adding external surfactant, capping agent or template. Biomolecules responsible for reducing Au^{3+} to Au^0 and stabilization of the resulting nanoparticles were extracted from the bark, and the synthesis was monitored for precursor concentration, percentage broth, pH of reaction media and reaction time. The biosynthesized nanoparticles were characterized using spectroscopic (FTIR and UV-Vis) techniques, advanced microscopic imaging (HRTEM, SEM/EDS), and Zeta potential measurements. Distinct color change from yellow to wine red was observed, indicative of the formation of gold particles at nanoscale. The SPR band was found at around 550 nm, in agreement with conventional synthetic protocols. The particles were stable with a net negative surface charge (–20 mV), a contribution associated with the protein nature of the broth. Addition of Pb^{2+} to the polydisperse nanoparticle suspension resulted in a color shift, to a faint blue color, coupled with a corresponding SPR shift to higher wavelengths, depending on the concentration of Pb^{2+} added. This color change is attributed to the aggregation of the colloidal particles due to complexation effects of the metal ions with the biomolecules on the surface of the nanoparticles.

Keywords: aggregation; broth; colorimetry; gold nanoparticles; Green Chemistry V; metals; *Moringa oleifera*; nanoparticles; SPR bands.

Introduction

The synthesis and application of different products of nanomaterials have received attention lately due to their novel properties, applications and the wide range of noble metals that can be utilized. Metal nanoparticles have found applications in biomedicine [1], catalysis [2], electronics [3] and in environmental applications [4]. These applications are premised on an understanding of the chemistry of the synthetic route so that different novel products can be produced from modeling the initial reaction conditions. Noble-metal nanoparticles have attracted extensive research interest due to their unique features such as optical, electronic, magnetic and catalytic properties [5].

For instance, gold nanoparticles are used extensively since they possess interesting physico-chemical properties such as biocompatibility [1], thermal stability [6], chemical stability, size related electronic, magnetic and optical properties [7], which then influence their application as sensors in environmental [5, 8]

Article note: A collection of invited papers based on presentations at the 5th international IUPAC Conference on Green Chemistry (ICGC-5), Durban (South Africa), 17–21 August 2014.

***Corresponding author: Peter P. Ndibewu,** Faculty of Science, Department of Chemistry, Tshwane University of Technology, Private bag X680, Pretoria, 0001, South Africa, e-mail: NdibewuP@tut.ac.za
Robert L. Mnisi and Ntebogeng S. Mokgalaka: Faculty of Science, Department of Chemistry, Tshwane University of Technology, Private bag X680, Pretoria, 0001, South Africa

and medical applications [1, 9]. The wide range of different applications imply that different properties are desired, therefore, the synthetic protocols employed vary significantly to produce gold nanoparticles of differing chemical properties.

Conventional chemical methods have been successful in synthesizing noble metal nanoparticles with all the desirable properties. These involve a reduction reaction of the precursor salt ($HAuCl_4 \cdot 3H_2O$) using appropriate reducing agents, principally tri-sodium citrate. However, these methods are usually expensive and the chemicals used may be toxic as they are likely to remain adsorbed on the surface of the nanoparticle [10]. Consequently, the resulting nanoparticles may be undesirable in biomedical and environmental applications [11]. For this reason, one of the most essential needs in nanotechnology is to develop environmentally benign and green approaches in metal nanoparticle synthesis.

Biological synthesis using microorganisms such as bacteria [12], fungi [13], algae [14] and yeast [15] have been reported, with limited success – due to the sensitivity of the microorganisms to changes to the external environment. Therefore, the use of natural, readily available, low-cost agro-wastes such as palm oil mill effluent (POME) [10], and plant mediated biosynthesis have received keen attention. The nanoparticles produced from these simple and eco-friendly synthetic protocols have morphologies that are comparatively similar to those synthesized from the conventional methods [16].

Various authors have reported on the successful plant-mediated reduction of the initial gold precursor salt using extracts from flowers [17], fruits [18], leaves [19], seeds [20] and barks [21]. However, to the best of our knowledge in literature, the use of *Moringa oleifera* plant parts for the synthesis of metal nanoparticles has not been reported. This is in spite of the widespread use of the plant for a wide variety of purposes, which are based on the amazing physicochemical properties reported in literature [22]. Therefore, this study explores and reports the potential use of *M. oleifera* broth extract in the biosynthesis of gold nanoparticles without the addition of capping agents, and their subsequent application to remove Pb^{2+} ions from synthetic aqueous solutions.

Experimental

Preparation of extract from *M. oleifera* bark

Moringa oleifera bark was collected from *M. oleifera* trees at the University of Botswana, Gaborone, southern Africa (Latitude: 24 39′ 40″, Longitude: 25 55′ 54″). It was washed with copious amounts of deionized water, thereafter air-dried. The bark was pulverized using an automated mechanical crusher to 300 μm through mechanical sieving. *Moringa oleifera* bark extract was obtained by boiling 40 g of the pulverized bark in 300 mL of deionized water for 20 min using a heated magnetic stirrer. The cooled extract was filtered under vacuum using Whatman filter paper (No. 41). This solution, always used fresh, was considered to be the stock *M. oleifera* broth solution and was used during the biosynthesis of Au nanoparticles.

Synthesis of gold nanoparticles with *M. oleifera* broth

Tetrachloroauric acid ($HAuCl_4 \cdot 3H_2O$) was used as the precursor salt, from which a concentration of 2.0 mM was prepared. Dilutions of the stock precursor salt solution were performed to obtain working concentrations for the different experiments. The synthesis was conducted by monitoring the effects of varying pH, percentage of *M. oleifera* broth, concentration of the precursor salt and synthesis time on the quality of the nanoparticles formed. Typically, the synthesis conditions were set at a volume ratio of 5:2 ($HAuCl_4 \cdot 3H_2O$ to *M. oleifera* broth) at pH 3.4, synthesis time and temperature of 60 min and 90 °C, respectively, 0.2 mM concentration of $HAuCl_4 \cdot 3H_2O$ and 300 rpm stirring rate, unless otherwise stated. Progressive reduction of Au^{3+} to Au^0 was visually monitored by a gradual color change from yellow, characteristic of the gold precursor salt, to a wine red color, indicative of the formation of colloidal gold nanoparticles.

The effect of pH on the quality of the synthesized nanoparticles was investigated by designing batch experiments with varying solution pHs, attained by adjusting the pH of the reaction media to pH 2, 4, 6, 8 and 10, by drop wise addition of 1.0 M HNO_3 or NaOH, depending on the desired pH. The effect of the initial concentration of the gold precursor ($HAuCl_4 \cdot 3H_2O$) salt was investigated by varying its concentration between 0.125, 0.25, 0.5, 1.0 and 2.0 mM in separate experiments. To study the effect of percentage (%) broth used, the broth was diluted with deionized water to provide percentage broth volumes of 100, 75, 50, 25 and 10 %, maintaining the $HAuCl_4$ volume at 50 mL. Effects of varying reaction time on the quality of the gold nanoparticles formed were investigated by taking 5 mL aliquots of the reaction mixture at pre-determined time intervals of 0, 5, 10, 15, 30 and 40 min using a pre-cleaned syringe. After each experiment, a portion of the colloidal suspension was cooled to room temperature, centrifuged at 14 000 rpm for 10 min and then frozen at −80 °C before freeze-drying them to obtain crystalline gold nanoparticles. The other aqueous portion was reserved for further experiments and characterization that require aqueous samples, such as TEM.

Characterization of synthesized gold nanoparticles

The gold nanoparticles were characterized for surface and spectral properties as well as size and shape determinations. Infra-red spectra were obtained using a PerkinElmer Spectro65 FTIR spectrometer (Perkin Elmer, Waltham, MA, USA), with 8 scans and 4 resolutions (cm^{-1}). A Micromeritics ASAP 2010 surface area and porosity N_2-BET analyzer (Micromeritics, USA) was used to determine the surface area and pore characteristics. Due to sample size limitations; BET analysis was done for the particles resulting from the 2.0 mM concentration of the precursor salt. Surface plasmon resonance (SPR) measurements were obtained using a Shimadzu UV-1601 spectrophotometer (Shimadzu, Kyoto, Japan) operated on 1 nm resolution. Size and morphological analyses were done using a JEOL-2100 high resolution transmission electron microscopy (HRTEM) (Akishima-Shi, Japan) operated at 200 kV. Samples were prepared by drop casting 5 μL on a 300 mesh carbon coated copper grid and allowed to dry at room temperature. Surface properties of the materials were determined using a JEOL JSM-7600F Field emission high resolution scanning electron microscope (HRSEM) coupled to an energy dispersive X-ray (EDX). Samples were adhered onto a conductive tape on the stub and mounted.

Zeta potential measurements were performed using a Malvern Zetasizer Nanoseries (Malvern, UK). Aqueous gold nanoparticle samples were diluted 1:20 parts in de-ionized water in a 12 mm glass cuvette. The cuvette was covered using a universal dip cell kit and placed into the sample compartment and the measurement performed.

Colorimetric determination of lead (Pb) ions in aqueous solutions

Metal ions in solution can be quantified by monitoring the aggregation behavior of the gold nanoparticles in the presence of these ions, which act as an external stimulus to the aggregation. This monitoring can be done visually; as gold nanoparticles tend to change color between their dispersed and aggregated forms, or spectrophotometrically through observations on the changes in the SPR bands between their dispersed and aggregated forms. In this section, both techniques were applied. Gold nanoparticles synthesized under different experimental conditions of pH, precursor concentration, broth amounts and different synthetic times were investigated for their aggregation behavior in the presence of Pb^{2+} ions, thereby determining the concentration of Pb. The aggregation behavior was investigated by adding, in triplicate, 800 μL of different concentrations of Pb (2.5, 5, 10, 25, 50 and 100 mM) to 500 μL of a Au nanoparticle colloidal suspension at room temperature (23 ± 2 °C) and pH 4.62 and then allowed to react for 24 h. The effect of pH was monitored by using Au nanoparticles synthesized under different pH conditions (pH 2, 4, 6, 8, 10), keeping all other parameters constant. Gold nanoparticles synthesized from different broth percentages were used to investigate their effect on the determination of Pb in aqueous solutions. This was done by taking triplicates of

500 µL of the different broth formulations (100, 75, 50, 25 and 10 %) and adding them to 800 µL of a 100 mM Pb and allowed to react for 24 h at room temperature (23 ± 2 °C) at pH 4.62. All analyses were done in triplicate and statistical estimations performed.

The resulting gold nanoparticle-metal complex was characterized using the same protocols as above. Spectral properties of this complex were investigated using a Shimadzu UV-1601 spectrophotometer to observe the SPR band behavior at different analytical conditions on the extent to which the wavelength shifts, corresponding to the degree of nanoparticle aggregation. A calibration curve was constructed from which analytical figures of merit, such as limits of detection (LOD), limits of quantification (LOQ), sensitivity, accuracy and linear range, were determined. The Student's t-test was performed on the data at 95 % confidence interval to rule out suspected outlier data points. A visual inspection was also performed on each experiment to observe any color changes from the initial wine-red to a faint blue color, characteristic of nanoparticle aggregation in the presence of Pb^{2+} ions.

Results and discussion

Reduction and stabilizing potential of *M. oleifera* biomolecules

Conventional synthetic methods for gold nanoparticles make use of chemical reagents, such as tri-sodium citrate and sodium borohydride, whose function is to facilitate the reduction of Au^{3+} to Au^{0} and to stabilize the resulting double layer gold nanoparticles through a surface charge. In this study, gold reduction and the subsequent stabilization of the nanoparticles was effected by the use of *M. oleifera* broth. The products of this synthesis and the mechanism thereof, in which this is achieved, is not documented in literature, hence the premise of this investigation.

Results from this investigation show that the broth of *M. oleifera* was able to reduce Au^{3+} to Au^{0}, resulting in the production of gold nanoparticles of significantly different sizes and shapes. The synthesis was monitored colorimetrically, and intermediate color changes (from yellow to wine-red. Fig. 1, insert) were observed and varied as a function of the initial synthesis conditions. This, together with other characterization techniques, proved the reduction potential of the broth in synthesizing gold nanoparticles.

The chemical composition of the broth is variable, but generally contains water soluble extractable biomolecules, such as proteins and carbohydrates. These are believed to have been responsible for the reduction and subsequent stabilization/capping of the nanoparticles. Preliminary characterization results on the elemental composition of *M. oleifera* bark (not presented here) show that it contains considerable quantities of nitrogen and sulfur, confirming earlier isolation and characterization results [23]. They found that cysteine ($C_3H_7NO_2S$) and methionine ($C_5H_{11}NO_2S$) occur in considerable amounts, and are therefore

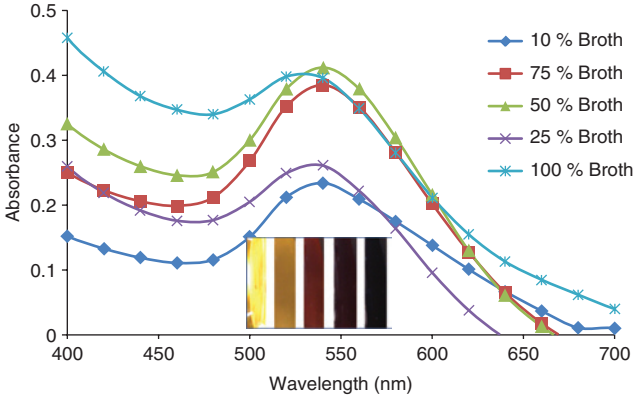

Fig. 1: FTIR spectra of green synthesized gold nanoparticles at different percentage volumes of the broth.

believed to have actively participated in the bioreduction of gold. The stabilization potential of the broth is believed to have been facilitated by the terminal thiol moiety to form the Au–S bond resulting in the formation of a negatively charged electric double layer on the surface of the gold nanoparticle. This agrees well with other findings [24] which suggested a dual role played by the amino group from the protein – as a reductant and as a capping agent.

Subsequently, other terminal functional groups such as carboxylate and amines are activated, which populated the surface of the nanoparticle thereby providing a protective layer of alternate functional groups. This is an important phenomenon, because this alternate arrangement masks the amines and prevents complete collapse of the nanoparticles through self-aggregation. Therefore the need to apply capping agents to prevent spontaneous aggregation of the nanoparticles, as is common practice when using other synthesis routes, is eliminated. However, some uncontrolled aggregation was observed due to the complex nature of the biomolecules, which would also allow undesired side reactions.

Zeta potential values give the surface charge of the nanoparticle, thereby indicating its stability and ability to react with other molecules. A threshold value of –20 mV is indicative of colloidal stability [25]. In the conventional synthesis of gold nanoparticles by the citrate reduction method, this surface charge is provided for by the citrate ions which populate the surface after reducing the gold. This citrate layer, with some chlorides (from the aqueous gold precursor) provides the capping that prevents aggregation, hence their stability. However, in this synthetic route, the negative charge is provided for by the water soluble functional groups which characterize the biomolecules. FT-IR spectra suggest that the broth contains functional groups such as carboxylates, alcohols, hydroxides and amines, wherein the relative amounts are dependent upon the concentration of the precursor concentration (Fig. 1). Zeta potential measurements show that some of the particles have potential values as low as –35 mV, depending on the initial synthesis conditions.

Effect of initial $HAuCl_4$ concentration on the formation of gold nanoparticles

The formation of nanoparticles could only happen when the precursor concentration is within a suitable range for nucleation to occur [10], and this range differs between different systems, hence the need to investigate specific cases. Figure 2 shows SPR bands for the synthesis of gold nanoparticles at different concentrations of the precursor salt.

The formation of gold nanoparticles results in a SPR band around 530 nm [26] in their dispersed state in solution. The UV-vis spectra (Fig. 2) show that precursor salt concentration is a determining factor in the formation of the nanoparticles, as the SPR band shifts to different wavelengths when the precursor concentrations is altered. Normally, small spherical gold nanoparticles exhibit a single surface plasmon band [27], a phenomenon that is clearly illustrated with 1 mM $HAuCl_4$ concentration. However, the other initial concentrations show that, even though the nanoparticles form, they tend to aggregate. This is evidenced by

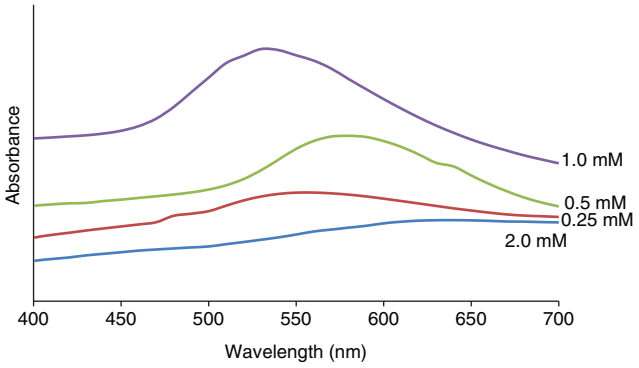

Fig. 2: UV-vis-NIR absorption spectra of gold nanoparticles synthesized at different initial concentrations of $HAuCl_4$ (2.0 mM, 1.0 mM, 0.5 mM, 0.25 mM and 0.125 mM).

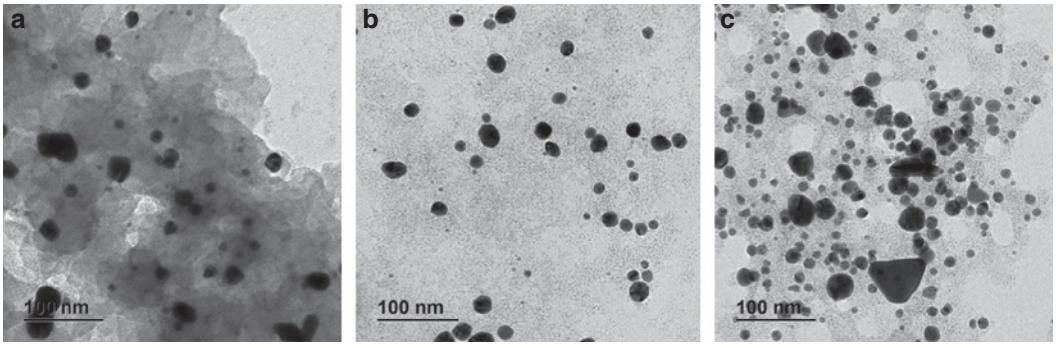

Fig. 3: TEM micrographs showing gold nanoparticles synthesized from 0.5 mM (a), 1 mM (b) and (c) 2 mM of $HAuCl_4$ salt.

SPR bands that occur at high wavelengths, and occasionally having shoulder regions, a characteristic feature of aggregated particles [23]. This suggests that small disperse gold nanoparticles were synthesized from the 1 mM $HAuCl_4$ salt concentration and the dispersed state is compromised with the other concentrations as some degree of agglomeration is evident.

The sizes of the nanoparticles varied greatly with the amount of precursor added. Transmission electron microscopy (TEM) micrographs show that as the precursor concentration is increased, there is a corresponding increase in the number of particles of different sizes (Fig. 3).

Effect of solution pH on the formation of gold nanoparticles

Within the context of the green synthesis of gold nanoparticles, a change in solution pH affects the reducing potential of the system in facilitating the reduction of Au^{3+} to Au^0. This phenomenon was investigated by altering the pH of the synthesis environment between pH 2 and 10, results of which are presented in Fig. 4.

The SPR bands are centered around 530 nm, which is the theoretical wavelength at which gold nanoparticles are formed, except when the solution pH is 4 where a higher wavelength was obtained. As the pH is decreased from pH 10 to pH 6, there is a corresponding increase in the absorbance, suggesting more particles are synthesized as the reaction medium is acidified. In fact, during the synthesis it was observed that as the pH became more basic (pH 6 to pH 10), it took more time for the appearance of the wine-red color. This implies that the synthesis is more favored in acidic media, as the absorption intensities are higher therein. However, as the solution medium becomes strongly acidic (pH 2), the SPR band shows the emergence of a shoulder at higher wavelength values which is indicative of the formation of nanoparticle aggregates – a phenomenon that has been observed previously [28]. This is attributed to the neutralization of the surface charge of the nanoparticle by the constant acidification of the reaction medium, which then increases the electrostatic attractions between adjacent particles, thereby reducing the hydrodynamic distance between them.

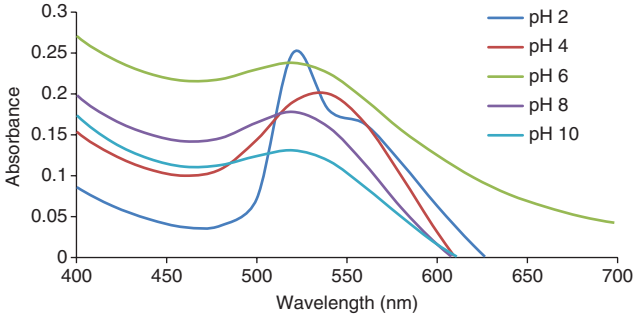

Fig. 4: UV-vis-NIR spectra of the gold nanoparticles synthesized at different pH conditions.

Conclusively, solution pH, initial precursor concentration and amount of broth are important parameters that define the biosynthesis of gold nanoparticles. The optimized experimental conditions presented herein culminated in gold nanoparticles of varying structural properties.

Colorimetric assay of P^{2+} ions based on the aggregation behavior of gold nanoparticles

Characterization of the aqueous AuNP–Pb complex in different synthesis conditions

Spectral properties of the gold nanoparticles after the addition of lead ions were investigated for the effect of precursor concentration, amount of broth and pH. SPR bands for the effect of precursor concentration on the aggregation of gold nanoparticles are presented in Fig. 5.

In the absence of Pb, the SPR band was at 530 nm (Fig. 5), which is characteristic of the formation of gold nanoparticles [28]. However, as metal ions were introduced into the system, the SPR peak shifted to higher wavelengths (from 530 nm to 540 nm), even though slightly. This is an obvious deviation from similar studies involving determination of metals, where the SPR band shifted to much higher wavelengths [23, 29]. The corresponding color change from wine-red was also very slight, giving a faint blue color for all the concentration ranges investigated. This faint color change is evidenced by a weak shoulder at 750 nm (Fig. 5), characteristic of a weakly aggregated colloidal suspension.

The position and magnitude of an absorption band is dependent on the size of the particles, the refractive index of the solvent used and the degree of aggregation of the nanoparticles [30]. TEM micrographs show that the gold nanoparticles, in the absence of the metal, depicted a degree of dispersity in solution (non-aggregated) and the average hydrodynamic radius was small; hence the absorption band was elaborate and broad [31]. However, as different concentrations of Pb were added (10 mM, 25 mM, 50 mM and 100 mM) there was a corresponding reduction in the inter-particle distance forming clusters or aggregates of metal-nanoparticle complex (Fig. 6a–d).

The introduction of the metal ions resulted in electrostatic attractions at the surface of the nanoparticle between the negatively charged gold nanoparticle surface and the positive metal ions. A weak ionic bond held by van der Waals forces results, which then pulls together the bulk of the surface molecules between adjacent nanoparticles. However, due to the size of the biomolecules on the surface, and the complex nature of the extraneous materials in the reaction medium, the net reduction in the inter-particle distance is minimized. The presence of terminal amino groups, which form strong metal chelates, enhances the coupling interactions between adjacent particles resulting in the collapse of the double layer on the nanoparticles.

The extent of the aggregation, and by extension the colorimetric determination, is affected by the sizes and shapes of the nanoparticles in solution. Size and shape of particles determine the optical properties of

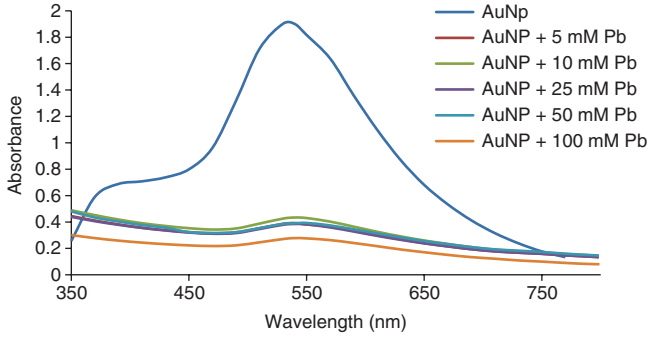

Fig. 5: UV-vis spectra of gold nanoparticles after the addition of varying concentrations of Pb.

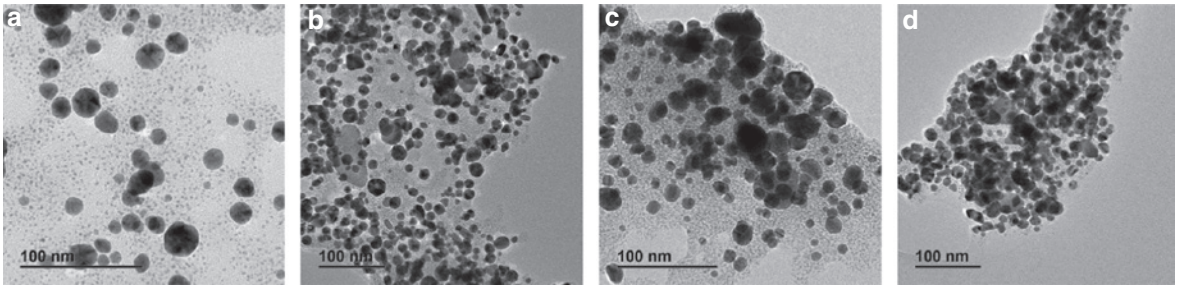

Fig. 6: TEM micrographs of gold nanoparticles after the addition of 10 mM, 25 mM, 50 mM and 100 mM of lead, respectively.

the bulk solution. In this study variable shapes (Fig. 7) and sizes (Fig. 8) of particles were obtained, which played a significant role in determining the extent of aggregation. Different shape options (triangular, elongated, and rectangular) are available as more of the broth is added to the reaction medium, until a threshold is reached, beyond which spherical nanoparticles are obtained [32]. More spherical shapes were obtained in this study, suggesting that the amounts of biomolecules added favored their formation rather the other size options.

Of note is that the density of the smaller sized nanoparticles was high in all the determinations, especially particles with diameters ≤10 nm. Normally, the formation of nanoparticles is a three stage process: a nucleation step, growth and then Ostwald ripening of the particles. The initial nucleation step is kinetically favored, since there is no requirement for the incipient surface energy [10]. This results in the formation of a scaffold on which the particles grow and is catalyzed by the bioorganic molecules in solution. However, due to supersaturation, the smaller particles are not dissolved back into solution to facilitate growth of large ones [10], but nucleation seems to be the predominant process, hence a large number of small particles are

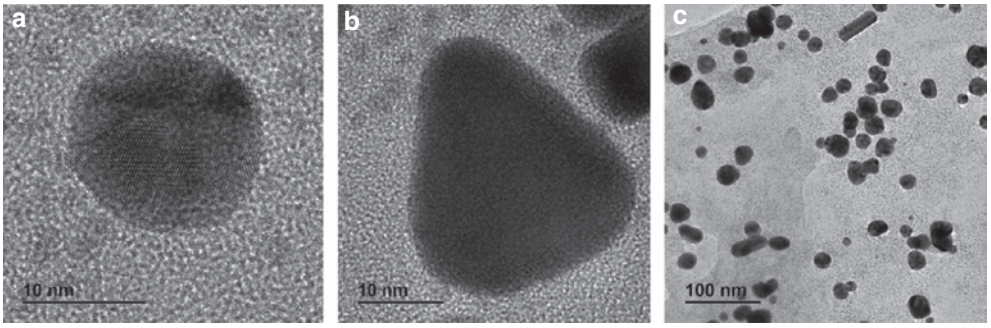

Fig. 7: TEM micrographs of colloidal gold nanoparticles showing different shapes: (a) spherical, (b) triangular and, (c) nanorods.

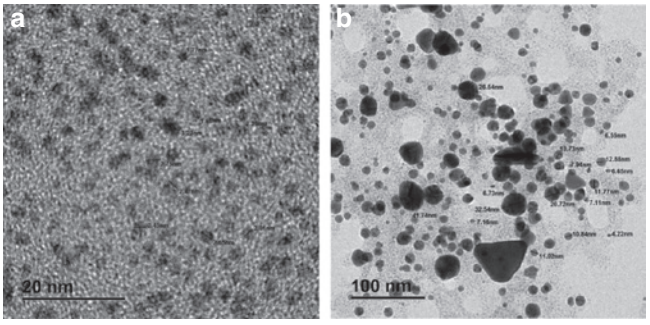

Fig. 8: TEM micrographs of colloidal gold nanoparticles showing different size ranges.

formed (Fig. 8a), and only a few of them dissolve back into solution, hence only a few larger ones are formed (Fig. 8b). The presence, in solution, of reducing/capping bioorganic molecules beyond stoichiometric equivalence makes this process possible. This also enables expedient capping/stabilization of the nanoparticles after synthesis so that the dissolution step is hindered. Some of the size differences can also be evident in the broadening of the SPR bands with an increase in the amount of broth added.

Spectrophotometric determination of lead in aqueous solutions

The amount of Pb in aqueous solutions can be determined using spectrophotometric techniques by making use of calibration curves. In this study, a method to determine the concentration of lead in aqueous solution was developed and monitored for the effect of pH, amount of broth and the concentration of initial precursor salt.

To evaluate the performance of the determination, analytical figures of merit were determined. A UV-vis spectrometer calibration curve is presented in Fig. 9, and shows good linearity ($r^2 = 0.9878$) over the calibration range (5.0–100 mM) for n = 5. Generally, percentage recoveries for the method were high (Table 1), even though the standard deviation appears to be high.

A Student's t-test performed on the recoveries for the lowest (5 mM) and highest concentrations (100 mM) at 95 % confidence level classifies them as outliers, hence the observed high standard deviation. These deviations can be attributed to the degree of aggregation induced by addition of these metal concentrations to the colloidal suspension. It appears that 5 mM did not provide stoichiometric equivalents of Pb to trigger enough electrostatic interactions with the terminal groups; hence the degree of aggregation was not significant. The detection limits (Table 2) of the method are therefore reported above the minimum standard concentration at 9.9 mM of Pb.

One major limitation in this study is the absence of the determination of tolerance limit of the technique in the presence of other metals with a potential interference effect on the spectrophotometric determination of lead. Additionally, the absence of data on the selectivity of the colorimetric technique in a multicomponent system means that the conclusions derived herein are only limited to a single component system. Current efforts are directed towards addressing these limitations.

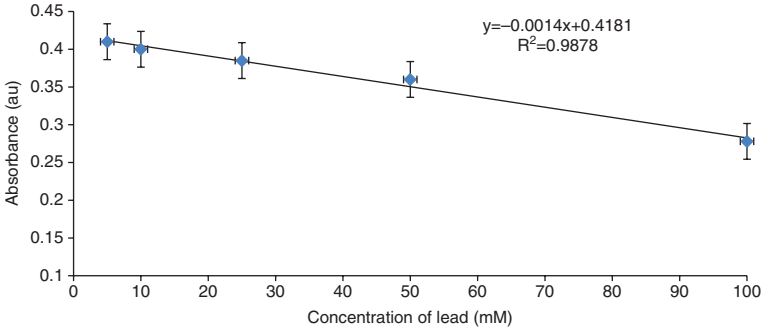

Fig. 9: Calibration curve lead standard solutions using a spectrophotometric technique.

Table 1: Percentage recoveries for the spectrophotometric determination of Pb.

Concentration (mM)	Recovery (%)
5	0.04
10	100
25	100
50	100
100	132

Table 2: Assay validation sheet for the spectrophotometric determination of Pb.

Parameter	Value (mM)
Accuracy	100 ± 16
Linear range	9.9–50 mM
LOD[a]	9.9 mM
LOQ[b]	30 mM
Sensitivity	0.418 au/mM

[a]Limits of detection; [b]limits of quantification.

Conclusions

The broth of *M. oleifera* contains some important biomolecules that are able to reduce gold, leading to the formation of gold nanoparticles. These nanoparticles are of variable shapes and sizes, a factor that is dependent upon the amount of broth. The complex water soluble bioorganic molecules in the broth were able to facilitate reduction of the gold and this reduction is dependent upon the concentration of the precursor salt, the pH and the amount of broth. These bioorganic molecules also stabilize the surface of the nanoparticles to some degree. However, at low pH values the nanoparticles aggregate, a major limitation if this property is to be explored for applications. The capping is believed to be through amino acid moieties, which *M. oleifera* bark is rich in. The presence of these also enhances the chelating potential of the nanoparticles so that they are able to bond to positively charged analytes, such as metals. The dispersion of these nanoparticles in solution is heterogeneous, with some degree of aggregation. This then limits colorimetric applications, since introduction of an analyte does not result in significant color changes, as the hydrodynamic distance between the particles is not significantly large. The determination of lead using spectrophotometry showed a potential, especially since no chemical capping agents were added. Good linearity was obtained, even though deviations were observed at low and high concentrations of the metal. In conclusion, it is shown in this study that green chemistry can be effectively used to hack nature via biomimicry of biosynthesis.

Acknowledgments: Financial support from the Tshwane University of Technology is acknowledged and appreciated.

References

[1] M. C. Daniel, D. Astruc. *Chemical Reviews* **104**, 807 (2004).
[2] C. T. Campbell, S. C. Parker, D. E. Starr. *Science* **298**, 811 (2002).
[3] S. A. Maier, M. L. Brongersma, P. G. Kik, S. Meltzer, A. A. Requicha, H. A. Atwater. *Adv. Mater.* **13**, 1501 (2001).
[4] P. G. Tratnyek, R. L. Johnson. *Nano Today* **1**, 44 (2006).
[5] B. Zargar, A. Hatamie. *Sens. Actuators, B.* **182**, 706 (2013).
[6] T. K. Sau, A. L. Rogach. *Adv. Mater.* **22**, 1781 (2010).
[7] N. Gupta, H. P. Singh, R. K. Sharma. *J. Mol. Catal. A*. **335**, 248 (2011).
[8] Y. Sun, Y. Xia. *Science* **298**, 2176 (2002).
[9] D. Zhang, O. Neumann, H. Wang, V. V. Yuwono, A. Barhoumi, M. Perham, J. D. Hartgerink, P. Wittung-stafshede, N. J. Halas. *Nanotechn. Lett*. **9**, 666 (2009).
[10] P. P. Gan, S. H. Ng, Y. Huang, S. F. Y. Li. *Bioresour. Technol*. **113**, 132 (2012).
[11] S. S. Shankar, A. Rai, A. Ahmada, M. Sastry. *Nat. Master.* **3**, 482 (2004).
[12] S. R. Rajasree, T. Y. Suman. *Asian Pac. J. Trop. Dis*. **2**, S796 (2012).
[13] M. E. Castro, L. Cottet, A. Castillo. *Mater. Lett.* **115**, 42 (2014).
[14] B. Sharma, D. D. Purkayastha, S. Hazra, L. Gogoi, C. R. Bhattacharjee, N. N. Ghosh, J. Rout. *Mater. Lett.* **116**, 94 (2014).
[15] G. Yamal, P. Sharmila, K. S. Rao, P. Pardha-Sardha. *Process Biochem*. **48**, 532 (2013).
[16] J. G. Parsons, J. R. Peralta-Vildea, J. L. Gardea-Torresdey. *Dev. Envir. Sc*. **5**, 463 (2007).
[17] V. K. Vidhu, D. Philip. 2014. *Spectrochim. Acta Part A.* **117**, 102 (2014).

[18] N. Basavegowda, A. Idhayadhulla, Y. R. Lee. 2014. *Industr. Crops Prod.* **52**, 745 (2014).
[19] S. P. Dubey, M. Lahtinen, M. Sillanpaa. *Colloids Surf. A*. **364**, 34 (2013).
[20] C. Jayaseelan, R. Ramkumar, A. A. Rahuman, P. Perumal. *Industr. Crops Prod.* **45**, 423 (2013).
[21] S. Yallappa, J. Manjanna, M. A. Sindhe, N. D. Satyanarayan, S. N. Pramod, K. Nagaraja. *Spectrochim. Acta Part A.* **110**, 108 (2013).
[22] A. Ndabigengesere, S. Narasiah, B. G. Talbot. *Water Res.* **29**, 703 (1995).
[23] N. Ding, H. Zhao, W. Peng, Y. He, Y. Zhou, L. Yuan, Y. Zhang. *Colloids Surf. A* **395**, 161 (2012).
[24] S. Boufi, A. M. Ferraria, A. M. B. Do Rego, N. Battaglini, F. Herbst, M. R. Vilar. *Carbohydr. Polym*. **86**, 1586 (2011).
[25] L. Sun, C. Tian, M. Li, X. Meng, L. Wang, R. Wang, J. Yin, H. Fu. *J. Mater. Chem. A* **1**, 6462 (2013).
[26] J. Turkevich, P. C. Stevenson, J. Hillier. *Discuss. Faraday Soc.* **11**, 55 (1951).
[27] S. L. Smitha, D. Philip, K. G. Gopchandran. *Spectrochim Acta Part A* **74**, 735 (2009).
[28] A. R. M. Salcedo, F. B. Sevilla III. *Phili. Sci. Lett.* **6**, 1 (2013).
[29] B. J. Kim, S. G. Oh, M. G. Han, S. S. Im. *Synth. Met.* **122**, 297 (2001).
[30] P. Mulvaney. *Langmuir* **12**, 788 (1996).
[31] S. Link, M. A. El-Sayed. *J. Phys. Chem. B* **103**, 8410 (1999).
[32] P. Chandra, M. Chaudhary, R. Pasricha, A. Ahmad, M. Sastry. *Biotechnol. Prog*. **22**, 577(2006).